Towards Scalable Within-Season Crop Mapping With Phenology Normalization and Deep Learning

Zijun Yang, Chunyuan Diao, and Feng Gao

***Abstract*—Crop-type mapping using time-series remote sensing data is crucial for a wide range of agricultural applications. Crop mapping during the growing season is particularly critical in timely monitoring of the agricultural system. Most existing studies focusing on within-season crop mapping leverage historical remote sensing and crop type reference data for model building, due to the difficulty in obtaining timely crop type samples for the current growing season. Yet the crop type samples from previous years may not be used directly considering the diverse patterns of crop phenology across years and locations, which hampers the scalability and transferability of the model to the current season for timely crop mapping. This article proposes an innovative within-season emergence (WISE) phenology normalized deep learning model towards scalable within-season crop mapping. The crop time-series remote sensing data are first normalized by the WISE crop emergence dates before being fed into an attention-based one-dimensional convolutional neural network classifier. Compared to conventional calendar-based approaches, the WISE-phenology normalization approach substantially helps the deep learning crop mapping model accommodate the spatiotemporal variations in crop phenological dynamics. Results in Illinois from 2017 to 2020 indicate that the proposed model outperforms calendar-based approaches and yields over 90% overall accuracy for classifying corn and soybeans at the end of season. During the growing season, the proposed model can give satisfactory performance (85% overall accuracy) one to four weeks earlier than calendar-based approaches. With WISE-phenology normalization, the proposed model exhibits more stable performance across Illinois and can be transferred to different years with enhanced scalability and robustness.**

***Index Terms*—Agriculture, crop mapping, crop phenology, deep learning, remote sensing, time series analysis.**

I. Introduction

FOOD security has been an increasing concern due to climate change and a growing global population [1], [2], [3]. To facilitate sustainable agricultural management, timely monitoring of agricultural systems is desired as it provides information and evidence for farmers and decision makers to better cope with environmental disturbances that may pose threats to crop production [4], [5], [6]. Among various characteristics of agricultural systems, crop type information is fundamental for a wide range of applications, including crop acreage estimation, crop yield, and production prediction [7], [8]. Within-season crop mapping is particularly critical because the timeliness of this information can help relevant stakeholders better estimate the upcoming trends in crop insurance, supply chains, and agricultural markets [7], [9].

The unprecedented advances in deep learning have opened up new opportunities for crop mapping with time-series remote sensing data [10], [11], [12], [13]. Recent studies have demonstrated that more favorable crop classification results can be obtained by deep learning models due to their abilities to automatically extract high-level intricate features from large amounts of time-series data [9], [14], [15], [16], [17]. Cai et al. [9] showed that the deep multilayer perceptron network performs better for crop mapping than conventional machine learning models when time-series band reflectance and vegetation index (VI) data were incorporated. Zhong et al. [16] found that the one-dimensional (1-D) convolutional neural network (1D-CNN) had superior performance over long short-term memory, support vector machine, and random forest models for identifying crop types with time-series VI inputs. Pelletier et al. [14] explored a temporal 1D-CNN (TempCNN) model for land cover classification in an agricultural area with time series of several VIs, and they found that the TempCNN model outperformed random forest and bidirectional gated recurrent unit models. Recently, attention mechanism has been found conducive to crop mapping with its ability to selectively emphasize more important temporal features [18]. These studies indicated that deep learning models can achieve promising crop mapping results, particularly with their abilities to model temporal dependencies in remote sensing time series.

While deep learning models have demonstrated promising performances in crop classification using whole-season time-series data, within-season crop mapping has its own challenge, i.e., the crop type information (ground reference data) is likely unavailable during the current growing season [19], [20], [21]. To address this issue, previous studies focusing on within-season crop mapping mostly utilized time-series remote sensing data in past growing seasons along with corresponding historical ground reference data for model training [9], [18], [22]. The pretrained model was transferred to the current growing season

Manuscript received 27 August 2022; revised 14 November 2022 and 1 January 2023; accepted 13 January 2023. Date of publication 16 January 2023; date of current version 24 January 2023. This work was supported in part by the National Science Foundation under Grant 2048068, in part by the National Aeronautics and Space Administration under Grant 80NSSC21K0946, and in part by the United States Department of Agriculture under Grant 2021-67021-33446.
(Corresponding author: Chunyuan Diao.)

Zijun Yang and Chunyuan Diao are with the Department of Geography and Geographic Information Science, University of Illinois at Urbana-Champaign, Urbana, IL 61801 USA (e-mail: zijuny2@illinois.edu; chunyuan@illinois.edu).

Feng Gao is with the Hydrology and Remote Sensing Laboratory, United States Department of Agriculture, Agricultural Research Service, Beltsville, MD 20705 USA (e-mail: feng.gao@ars.usda.gov).

This article has supplementary downloadable material available at https://doi.org/10.1109/JSTARS.2023.3237500, provided by the authors.

Digital Object Identifier 10.1109/JSTARS.2023.3237500

for the prediction of crop types, based on the assumption that crop phenological dynamics on the same calendar dates in different years are comparable. However, crop phenology is not only a function of crop species, but also a reflection of various environmental and management conditions such as temperature, precipitation, soil properties, and planting date. The same crop species can exhibit diverse interannual changes in its phenological dynamics [23], [24], [25]. Such calendar-based models are, thus, inherently limited as they do not take the spatiotemporal variation of crop phenological dynamics into consideration. When disturbances happen and the phenological patterns are shifted in the time dimension, those calendar-based models may be less robust and hard to generalize. Recent literature demonstrated the potential of leveraging crop phenology information in helping normalize crop growth patterns over space and time [26]. Thus, the incorporation of interannual phenology information will be a promising way to enhance the model scalability.

Crop phenology characterization using time-series remote sensing data has been explored in recent years, yet within-season crop phenology detection remains a challenging task [27], [28]. With time-series VI curves, crop phenology was derived by phenophase extraction methods in terms of curve characteristics (e.g., predefined threshold, curve derivative, and curvature change rate) and phenology matching models (e.g., shape model and hybrid phenology matching model) [29], [30], [31], [32], [33], [34], [35], [36]. However, those abovementioned methods were mostly designed with whole-season VI curves, which made them hardly applicable within the growing season [27]. Recent advances in within-season crop phenology characterization (e.g., timely crop emergence date estimation using the within-season emergence method) may provide us with new opportunities to explore innovative approaches that integrate within-season crop phenology information into crop mapping, holding potentials to improve the scalability and robustness of crop mapping models [27], [28], [37]. Yet such integration of within-season crop phenology is still underexplored in current studies.

In this article, we propose an innovative within-season emergence (WISE) phenology normalized deep learning model towards scalable within-season crop mapping. Through the incorporation of crop phenology, we aim to develop a model that is more scalable and can be transferred to different years while maintaining satisfactory accuracy.

II. Study Site and Materials

The state of Illinois in the U.S. is selected as our study site [see Fig. 1(a)]. Illinois is a leading agricultural state in the U.S. Located in the Corn Belt, Illinois is predominantly planted with corn and soybeans, which are the two crop types considered in crop mapping. The study site spans from 37° to 42.5° north and from 87.5° to 91.5° west. As a result, the environmental conditions vary throughout the state. Illinois is divided into nine agricultural statistics districts (ASDs), with each ASD consisting of counties of comparable agricultural characteristics [see Fig. 1(b)]. The interannual variations of crop phenological dynamics are substantial [see Fig. 1(c)]. Crop emergence dates

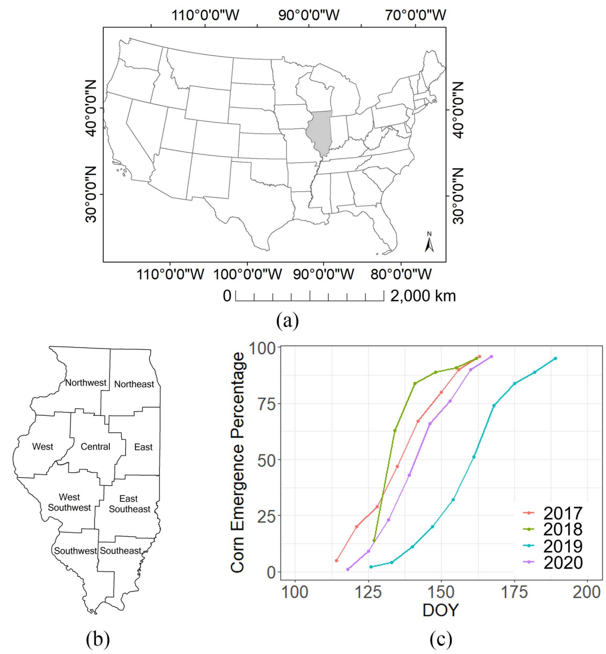

Fig. 1. (a) Study site of Illinois (in gray). (b) Nine ASDs in the state of Illinois. (c) Cumulative percentages of corn emergence from 2017 to 2020 from Illinois crop progress reports (CPRs). Substantial interannual variations in crop emergence can be observed.

in Illinois have also been found to be with larger interannual variations compared to other states in the U.S. Corn Belt [28]. Therefore, Illinois is ideal for testing model scalability and transferability across different years.

The MODIS MCD43A4 Version 6 products are utilized in this article. The MODIS MCD43A4 products are nadir Bidirectional Reflectance Distribution Function-adjusted daily images with a spatial resolution of 500 m. These temporally dense data with minimal cloud cover build a solid foundation for crop phenology characterization and the subsequent crop mapping. Six bands of the MODIS products are used for crop mapping, namely blue, green, red, near-infrared (NIR), short-wave infrared 1 (SWIR1), and SWIR2 bands. Normalized difference vegetation index (NDVI) is also derived from the MODIS data for crop phenology characterization and crop type mapping. The snow quality layer of the MODIS MCD43A2 data is used to exclude the pixels contaminated by snow.

With a 500-m spatial resolution, one MODIS pixel may encompass multiple land covers. Thus, we employ the cropland data layer (CDL) dataset to identify "pure" pixels for corn and soybeans. The CDL dataset consists of maps of major crop types at 30-m spatial resolution, produced and published annually by National Agricultural Statistics Service (NASS), United States Department of Agriculture (USDA) [38].

Crop progress reports (CPRs) published by USDA NASS provide weekly updates on cumulative proportions of major crop species (e.g., corn or soybeans in Illinois) that are at different phenological stages within the state during the growing season [39]. In this article, we utilize the emerged percentages of corn and soybeans from CPRs in Illinois as the state-level crop phenology information (see Fig. S1). The median dates of various phenological stages recorded in CPRs are shown in Table SI.

III. Methodology

A. Overview

In this article, we propose a WISE-phenology normalized deep learning model for scalable within-season crop mapping. Time-series NDVI generated from pure pixels in the MODIS data will be input into the WISE algorithm. The WISE-derived crop emergence dates are used for normalizing time-series remote sensing data, which are then utilized for training the deep learning-based crop mapping model. Attention-based 1D-CNN (At1DCNN) is employed in this article to conduct within-season crop mapping due to 1D-CNN's reliable performances and computational efficiency [14], [16] and attention module's ability to better learn temporal features [18]. To test the effectiveness of the proposed WISE-phenology normalization approach, we compare the proposed approach with two other approaches: the calendar-based approach without phenology normalization, and the CPR state-level phenology normalization approach.

B. Data Preparation

To identify pure pixels, the CDL data are resampled to the MODIS spatial resolution. Pure pixels are defined as resampled pixels with percentages of corn or soybeans over 90%, and are used to produce time-series reflectance and NDVI data. Extreme reflectance and NDVI values (i.e., out of three times of standard deviation) are removed and linearly interpolated using the corresponding temporally nearest valid observations. Fig. S2 shows the distribution maps of the pure pixels for corn and soybeans across Illinois. In total, 39239, 39133, 33664, and 38682 pure pixels are identified in 2017, 2018, 2019, and 2020, respectively. The percentage of the corn pure pixels ranges from 48.78% to 51.98%, and the percentage of the soybeans pure pixels is from 46.63% to 51.22% (see Table SII).

C. WISE-Phenology Normalization

The WISE algorithm was developed to identify crop emergence dates within the growing season. As Fig. 2(a) shows, a local moving Savitzky–Golay (SG) filter is first used to detect and remove extreme values in the NDVI time series and then smooth the data. Gaps are filled by a polynomial function, which is fitted using the nearest five valid observations. This design allows filling large gaps when valid observations are sparse and also preserving local patterns when observations are dense.

The moving average convergence divergence (MACD) function [40] is employed to detect the early trends of crop green-up. The MACD is generated by calculating the difference between a short-term exponential moving average (EMA) and a long-term EMA. EMA and MACD are defined as follows:

$$\mathrm{EMA}\ (v(t),\ n) = v(t) * k + \mathrm{EMA}(v(t-1), n) * (1-k), \tag{1}$$

$$k = 2/(n-1), \tag{2}$$

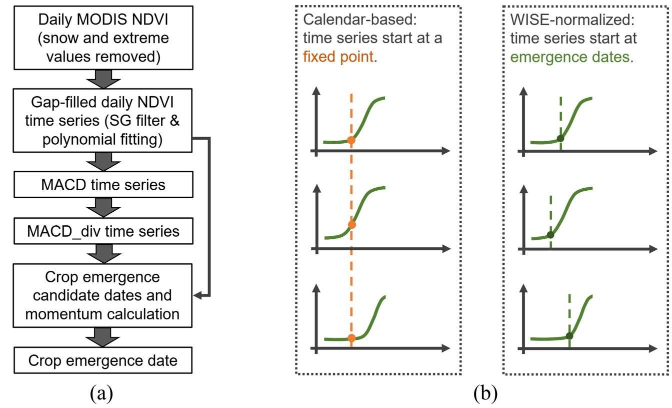

Fig. 2. (a) Flowchart for the WISE algorithm. (b) Illustrative diagram of the WISE-phenology normalization process.

$$\mathrm{MACD}\ (t) = \mathrm{EMA}(v(t),\ a) - \mathrm{EMA}(v(t), b), \tag{3}$$

where $v(t)$ stands for the NDVI time series; n stands for the moving window size that is used for the calculation of EMA; k is the weight given to the most recent observation, regulated by the moving window size. The MACD function is the difference between two EMAs with different window sizes, in which a and b represent the two sizes of moving windows for the shorter-period and longer-period EMA, respectively. Here, a and b are set to be 5 and 10, respectively. The MACD results are correlated with the changing trends in the NDVI time series. For example, a change from negative to positive values of MACD in the early season indicates a change to an uptrend in NDVI. Considering that moving averages are involved in the calculation of MACD, the trend change in MACD can be later than the actual trend change in the NDVI time series. MACD divergence (MACD_div) is, thus, introduced to capture early trend changes and is defined as follows:

$$\mathrm{MACD\_div}(t) = \mathrm{MACD}(t) - \mathrm{EMA}(\mathrm{MACD}(t), c), \tag{4}$$

where c stands for the window size, set to be 5 in this article. The emergence date t is detected when following criteria are met:

$$\mathrm{MACD\_div}(t-1) < \mathrm{MACD\_div\_threshold}$$

and

$$\mathrm{MACD\_div}(t) > \mathrm{MACD\_div\_threshold}$$

and

$$\mathrm{MACD}(t) < \mathrm{MACD\_threshold}, \tag{5}$$

where MACD_threshold and MACD_div_threshold are predefined thresholds, set to be 0.01 and 0, respectively [27], [28].

As early-season crop green-up trends are often subtle and confused with noises caused by soil background or weeds growth, the WISE algorithm incorporates the momentum of green-up to ensure the significance of the NDVI uptrend. The momentum is calculated by the cumulative positive MACD since the detected potential emergence date divided by the number of days after the potential emergence. A threshold of 0.01 is adopted in this article. For each year and crop type, the WISE results are further

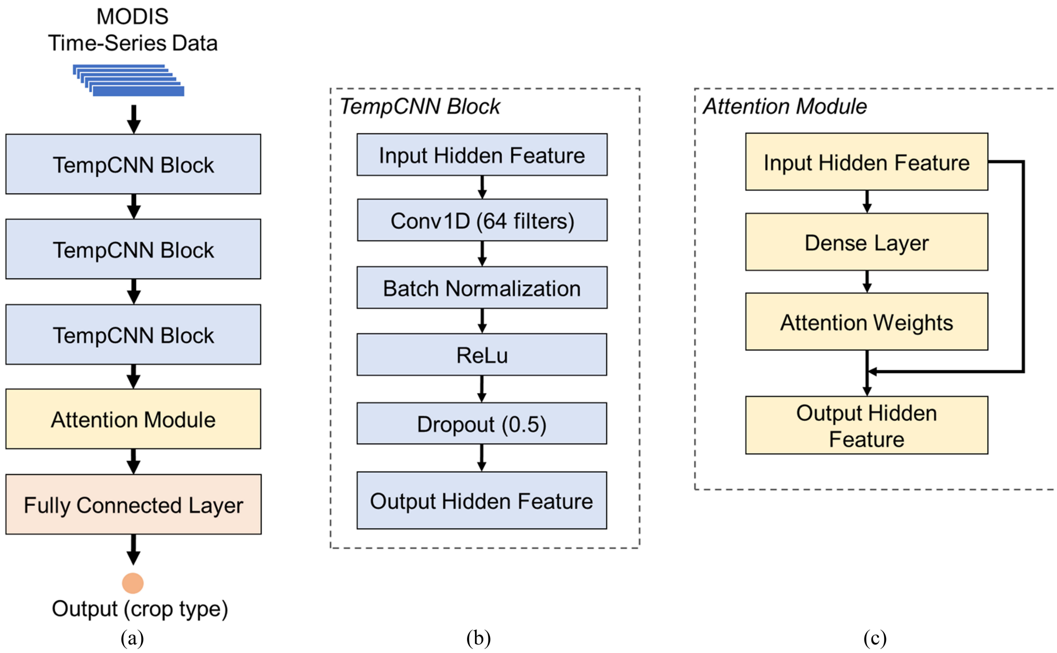

Fig. 3. (a) Model architecture of the At1DCNN model. (b) Structure of the TempCNN block. (c) Structure of the attention module.

summarized and adjusted by a constant value determined by the difference between the median WISE emergence date and the corresponding median CPR emergence date. All the parameters (i.e., a, b, c, MACD_threshold, and MACD_div_threshold) in WISE are tuned in consideration of a range of values with reference to previous studies [27], [28].

To ensure that the reflectance of the same crop type can be compared over space and time, time-series remote sensing data are normalized by the WISE-derived within-season crop phenology information. Fig. 2(b) illustrates how the WISE-phenology normalization is conducted. An estimated crop emergence date is given to each pixel by the WISE algorithm. When used for model training and prediction, each pixel's time-series observations are adjusted by starting from its emergence date, instead of the same fixed start date. Therefore, the WISE-phenology normalization approach can align the early-season crop phenology across different locations and years, helping accommodate the spatiotemporal variations in crop phenological dynamics.

D. Deep Learning Classifier

The At1DCNN model consists of three TempCNN blocks, an attention module, and a fully-connected output layer (see Fig. 3). The TempCNN blocks can automatically extract and learn temporal patterns by convolving the input time series with 1-D filters. Each TempCNN block contains a 1-D convolutional layer with 64 filters and a kernel size of 5, followed by batch normalization, rectified linear unit (ReLU) activation, and a dropout layer with a dropping probability of 50% [see Fig. 3(b)]. Batch normalization and ReLU activation are used to help speed up the convergence of the network and allow the model to learn more complex features. Dropout can alleviate the overfitting issue by randomly excluding a certain percentage of neurons. The attention module is utilized to optimize the contributions of learned hidden features through multiplying the hidden features by attention weights, which are generated by a dense layer with a Softmax activation [see Fig. 3(c)]. The output hidden features are then input into a fully-connected layer with 128 neurons, followed by the output layer with a Softmax activation, which gives the classification results.

The At1DCNN model is implemented using the Keras library with a Tensorflow backend. The model is trained on an NVIDIA Tesla P100 GPU. An Adam optimizer with adaptive learning rates is used, with the initial learning rate set as 0.001. The number of epochs is set to be 20. The hyperparameters (i.e., number of filters, kernel size, dropout probability, number of hidden neurons, and training epochs) in the At1DCNN are tuned and determined with reference to relevant studies [14], [16].

E. Experiment Design

Time-series remote sensing data from 2017 to 2020 in Illinois are collected in this article. The dataset contains two crop types: corn and soybeans. To test the robustness of the WISE-phenology normalization approach, we first only use the 2017 data as the training data, instead of using data collected from multiple years. The trained model will be tested for predicting crop types in 2018, 2019, and 2020. To further assess the scalability of the WISE-phenology normalization approach, the crop mapping results are analyzed across the nine ASDs in Illinois. As 2019 is known for the occurrence of extreme precipitation events in spring, crop planting is substantially delayed in that year. Thus, we conduct another round of experiments with that "abnormal" year data as the training data, and the other three years (2017, 2018, and 2020) are used for the testing purpose.

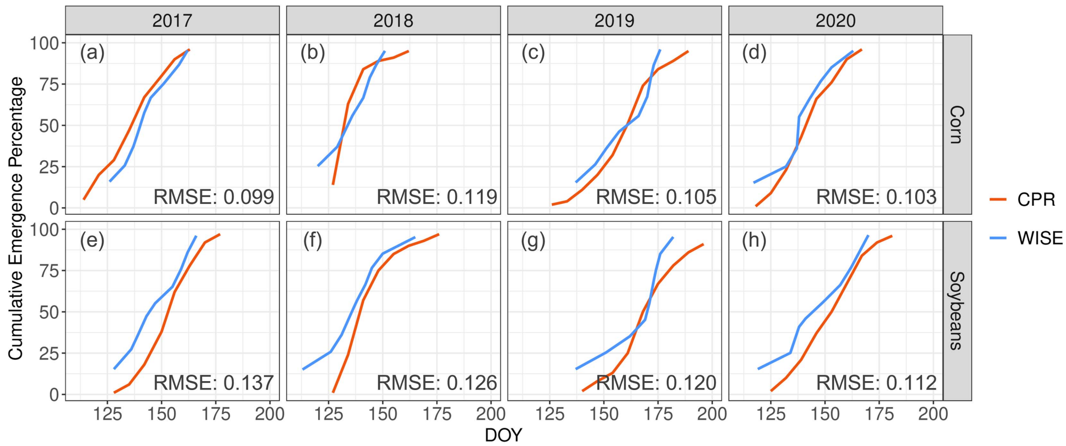

Fig. 4. Cumulative percentages of WISE-derived crop emergence dates (blue) versus CPR-based crop emergence dates (red) for corn [(a) to (d)] and soybeans [(e) to (h)] from 2017 to 2020 in Illinois.

Three approaches are compared to test the effectiveness of the WISE-phenology normalization method: 1) calendar-based approach without phenology normalization, 2) CPR state-level phenology normalization, and 3) WISE-derived pixel-level phenology normalization. For approach 1, all the time series in all the years share the same start date on day of year (DOY) 120, with the growing season in Illinois usually starting from late April. For approach 2, all the time series in the same year share the same start date as the median crop emergence date indicated by the CPR in that year. For approach 3, each pixel has its own start date estimated by the WISE algorithm. For all approaches, time series are sampled every seven days since their start dates.

To examine how model performances change during the growing season, we test crop mapping with different lengths of time-series remote sensing data acquired from the start date to DOY 150, 157, 164, …, 332, respectively. For the experiments with 2017 as the training year, overall accuracy and F1 scores for each crop type are selected as the accuracy metrics to assess the model performances. Overall accuracy is employed for evaluating overall model performance. F1 score is the harmonic mean of producer's accuracy and user's accuracy, which can be used to assess the model performance for each crop type [41]. The coefficient of variation (CV) of the overall accuracy across the nine ASDs is utilized to assess the consistency of the model performance across districts with different climatic conditions. The predicted probability of each crop type from the At1DCNN model is also examined throughout the growing season for a better understanding of the model performances. For the experiments using 2019 as the training year, overall accuracy is examined to further test the model robustness.

IV. Results

A. WISE-Derived Phenology

The cumulative percentages of the WISE-derived crop emergence dates for corn and soybeans are derived and compared with the corresponding CPR data (see Fig. 4). The cumulative percentages of the WISE-derived crop emergence dates (cyan lines) are generally well aligned with the cumulative emergence percentages recorded in CPR (red lines) for both corn and soybeans from 2017 to 2020. Consistent with Fig. 1(b), the WISE algorithm successfully detects the delayed crop emergence in 2019 and relatively early emergence in 2018. The root-mean-square error values between the estimated and corresponding CPR percentages are around 10%. Overall, the results suggest that the WISE algorithm can effectively capture the spatiotemporal variation in crop emergence throughout the state of Illinois.

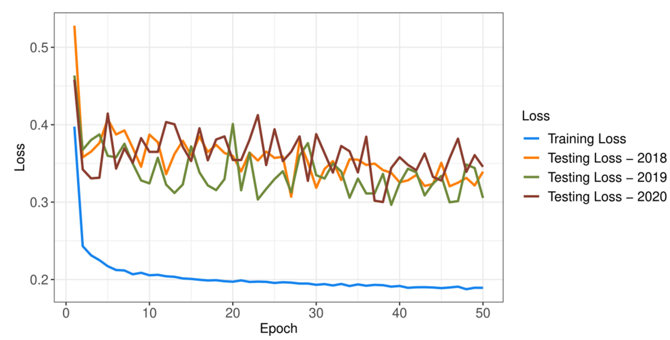

Fig. 5. Training and testing loss of the WISE-phenology normalized model at the end of the growing season using the whole-season time-series data.

B. Crop Classification Results

Fig. 5 shows the training and testing loss of the WISE-phenology normalized model trained with the whole-season time-series data (i.e., from the WISE-derived crop emergence to the end of the season), with 2017 as the training year. The training loss decreases smoothly and converges with the increasing number of epochs. The testing loss curves show a general trend of decreasing and convergence with fluctuations. The testing loss is also generally higher than the training loss, as the model is tested in years different from the training year.

Fig. 6 and Table I demonstrate how performances of the At1DCNN model change during the growing season under

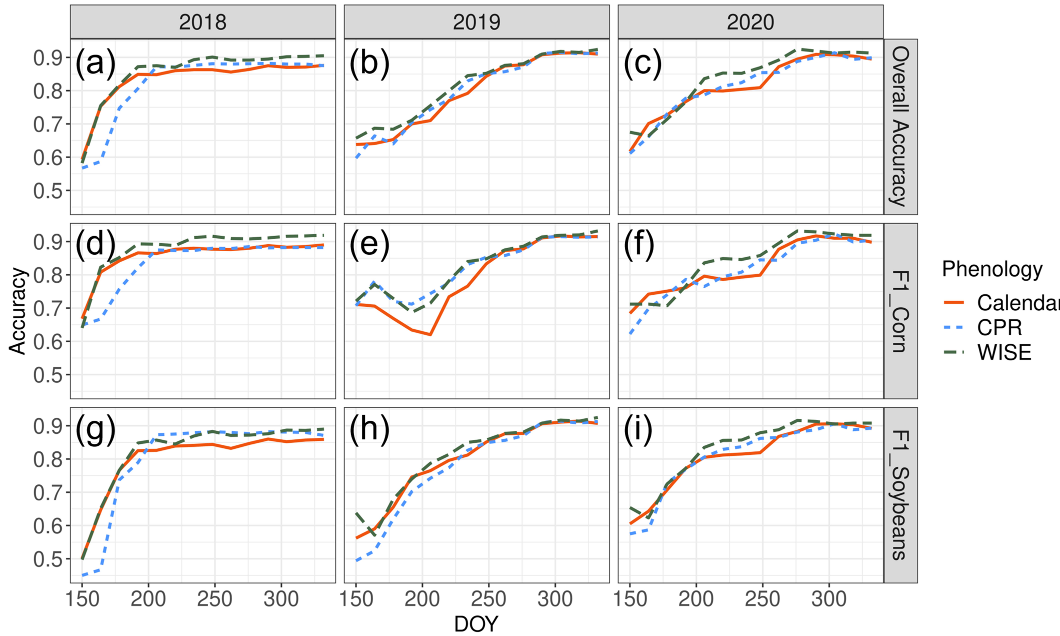

Fig. 6. Accuracy assessments of the crop classification results generated by the WISE-phenology normalized model (dark green), CPR normalized model (blue), and calendar-based model (red), using 2017 data for training. (a)–(c) Overall accuracy throughout the growing season from 2018 to 2020. (d)–(f) F1 scores for corn throughout the growing season. (g)–(i) F1 scores for soybeans throughout the growing season.

TABLE I
OVERALL ACCURACY FOR DIFFERENT PHENOLOGY APPROACHES USING VARYING LENGTHS OF TIME SERIES

Year	Time	Overall Accuracy		
		Calendar	CPR	WISE
2018	End of June	81.2%	74.7%	**81.7%**
	End of July	85.4%	**87.3%**	87.0%
	End of August	86.3%	87.9%	**89.7%**
	End of Season	87.6%	87.5%	**90.5%**
2019	End of June	65.3%	64.0%	**68.4%**
	End of July	74.0%	75.9%	**78.8%**
	End of August	81.8%	83.0%	**84.9%**
	End of Season	91.0%	91.3%	**92.4%**
2020	End of June	72.7%	**73.0%**	71.4%
	End of July	80.0%	79.7%	**84.5%**
	End of August	80.7%	83.4%	**86.1%**
	End of Season	89.5%	89.9%	**91.3%**

different phenology approaches from 2018 to 2020. At the end of the season, the WISE-phenology normalized model achieves higher overall accuracy in all the three years (90.5% in 2018, 92.4% in 2019, and 91.3% in 2020) and outperforms the calendar-based (87.6% in 2018, 91.0% in 2019, and 89.5% in 2020) and the CPR normalized models (87.5% in 2018, 91.3% in 2019, and 89.9% in 2020). The proposed model also gives higher F1 scores for both corn and soybeans at the end of the season in the three testing years [see Fig. 6(d)–(i)]. Though performing worse than the WISE-phenology normalized model, the CPR normalized model exhibits better performance than the calendar-based model at the end of the season. While we only use one year (2017) for training, it is noted that the proposed model performs well in all three testing years (2018–2020), confirming the scalability and robustness of the model.

As indicated by Fig. 6 and Table I, our proposed model also demonstrates its advantages throughout the growing season, although the patterns in different years may vary. Taking the overall accuracy in 2018 as an example, Fig. 6(a) shows that the WISE-normalized model and the calendar-based model give comparable performances initially in 2018; both are better than the CPR normalized model (from DOY 150 to around 180). After DOY 180, the WISE-phenology normalized model gains a consistent advantage over the other two models until the end of the season; the CPR normalized model also performs better than the calendar-based model since around DOY 200. In 2019 [see Fig. 6(b)], our proposed model gives better results throughout the growing season, with the advantage being more considerable in the early half of the growing season. The CPR normalized model mostly performs better than the calendar-based model but worse than the WISE normalized model. In 2020 [see Fig. 6(c)], the three models perform comparably at the beginning of the growing season. The proposed model performs better since around DOY 190, while its advantage is more obvious in the mid- to late-season until around DOY 280 compared to the end of the season. In terms of the F1 scores, the WISE-phenology normalized model also shows considerable advantages over the other two models in most cases, i.e., classifying corn in 2018 and 2020 and classifying soybeans in 2019 and 2020.

Figs. 7 and 8 show the monthly evolution of predicted probability generated by the proposed model for corn and soybeans pixels, respectively. Table SIII reports weekly median values of the predicted probabilities for corn and soybeans pixels. Pixels with a predicted probability over 0.5 are correctly classified, and a higher predicted probability suggests higher confidence of the model in predicting a pixel as corn or soybeans. As the

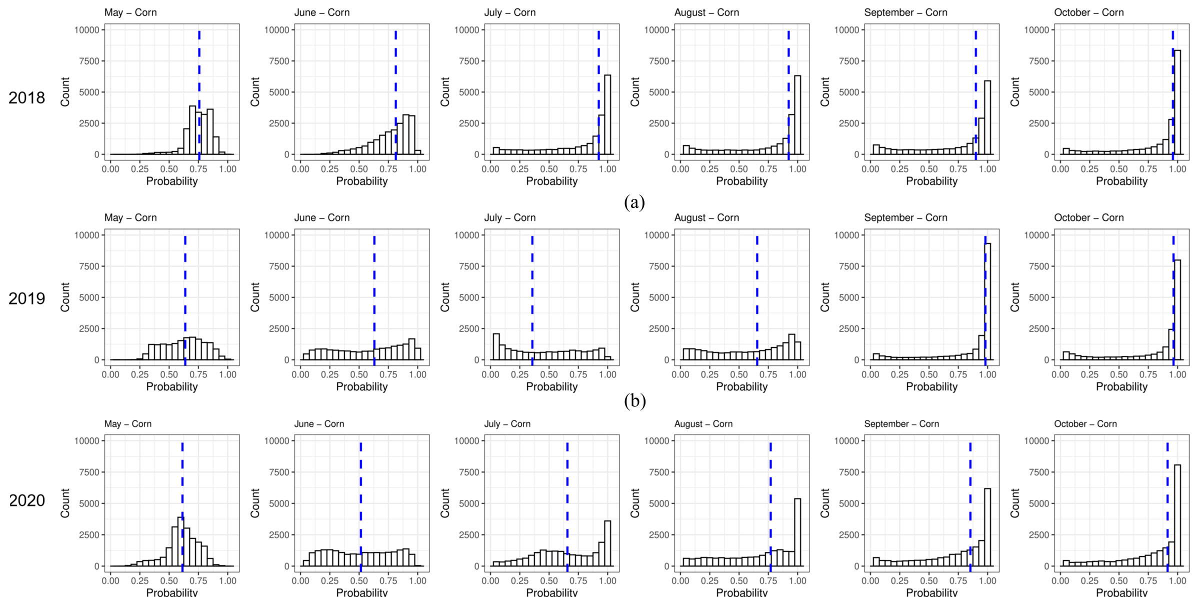

Fig. 7. Histograms of predicted probability for corn pixels from the end of May to the end of October, generated by the WISE-phenology normalized model in (a) 2018, (b) 2019, and (c) 2020, with 2017 data for training. Dashed lines represent the median of predicted probability. Higher probability values indicate that the model has higher confidence in its predictions of crop types.

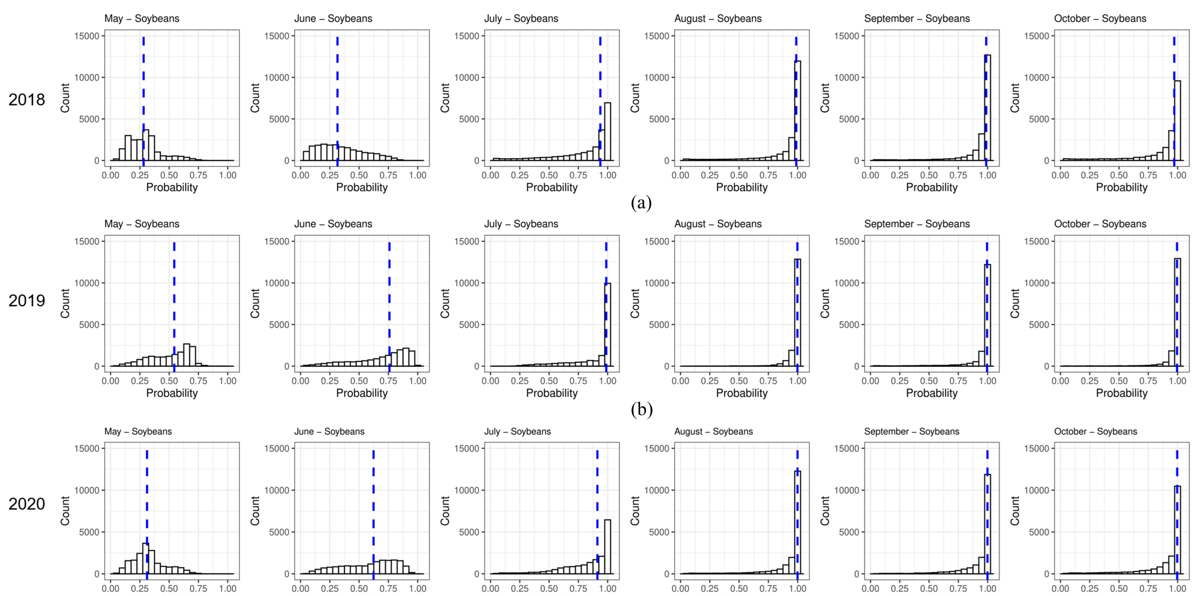

Fig. 8. Histograms of predicted probability of soybeans pixels from the end of May to the end of October in (a) 2018, (b) 2019, and (c) 2020, generated by the WISE-phenology normalized model with 2017 data for training. Dashed lines represent the median of predicted probability. Higher probability values indicate that the model has higher confidence in its predictions of crop types.

growing season progresses, more pixels are correctly classified and predicted with higher predicted probability. For corn, our model can detect most corn pixels starting from the end of July in 2018 and 2020 [see Fig. 7(a) and (c)]. In 2019, due to the delayed crop phenology, the model may accurately identify corn pixels only after the end of August. For soybeans, the model is able to identify most soybeans pixels since the end of July in all the three testing years (see Fig. 8).

Fig. 9 shows the monthly classification maps from the end of May to the end of October in the three testing years, and Fig. S3 shows the monthly classification maps, which are focused on the Central ASD in Illinois. Both figures suggest that the model is able to capture the general patterns of the distribution of corn and soybeans by the end of July in 2018 and 2020, though the model might overestimate the proportions of soybeans at that time. The overestimation of soybeans is consistent with the

Fig. 9. Classification maps by the end of May, June, July, August, September, and October generated by the WISE-phenology normalized model in (a) 2018, (b) 2019, and (c) 2020, along with the reference maps in corresponding years.

histograms of predicted probability: Figs. 7 and 8 show that the median predicted probability for corn is lower than that for soybeans by the end of July in those two years, and the number of corn pixels misclassified as soybeans is larger than the number of soybeans pixels misclassified as corn. In 2019, the model starts capturing the general patterns of crop distributions from the end of August. In general, the classification results become more similar to the reference map as the growing season progresses.

Tables I and II show quantitative measures on how the models perform during the growing season. Table I shows the overall accuracy by the end of June, July, and August for the three approaches in all the testing years. The WISE-phenology normalized model achieves the best performance in most cases.

TABLE II
DOY OF OVERALL ACCURACY REACHING 85% FOR DIFFERENT PHENOLOGY APPROACHES

Year	DOY		
	Calendar	CPR	WISE
2018	208 (July 27)	201 (July 20)	**189 (July 8)**
2019	251 (Sep. 8)	247 (Sep. 4)	**245 (Sep. 2)**
2020	254 (Sep. 10)	243 (Aug. 30)	**218 (Aug. 5)**

The only exceptions are the end of July in 2018 and the end of June in 2020, when the CPR normalized model performs the best among the three models. It is also noted that the CPR normalized model generally yields higher overall accuracy than the calendar-based model, which suggests that state-level phenology normalization can also help with more accurate crop mapping. While we might obtain less satisfactory results by the end of June, our proposed model gives an overall accuracy around 85% in both 2018 (87.0%) and 2020 (84.5%) by the end of July. In 2019, the within-season accuracy is relatively lower due to the delayed planting and emergence in that year [see Fig. 1(b)]. Yet an overall accuracy of 80% can still be obtained around the beginning of August using the WISE approach [see Fig. 6(b)].

Using 85% as a threshold of satisfactory overall accuracy, Table II presents how early the crop mapping models can generate satisfactory results. DOYs within the seven-day sampling intervals are estimated through linear interpolation. The WISE-phenology normalized model reaches an 85% overall accuracy earlier than the other two models in all three testing years. The CPR normalized model also gives satisfactory results earlier than the calendar-based model. The interannual patterns in the results are consistent with Fig. 1(b), i.e., crops were planted the earliest in 2018 and the latest in 2019 among the three testing years. Similarly, the models achieve satisfactory results relatively earlier in 2018 but much later in 2019. Overall, the WISE-derived within-season phenology is conducive to better performances of crop mapping models within the growing season.

As 2017 is selected as the training year, 2018 and 2019 are the two testing years with early and late crop emergence, respectively, whereas 2020 is assumed to be a year that is more similar to the training year in terms of crop phenology. While Tables I and II indicate that the timing of crop emergence will affect how early the models yield accurate results, we do observe that 2020 may not guarantee a higher end-of-season accuracy. Though excessive precipitation in spring 2019 leads to the lower accuracy for early- to mid-season in that year, the models also achieve higher end-of-season accuracy in 2019 (see Table I). This observed pattern is likely resulted from the fact that other factors throughout the growing season (e.g., phenology development in the middle to late season) can also affect crop classification accuracy.

To better understand how crop emergence information might affect the model performances, all the pure pixels are divided into four quantiles based on their WISE-derived emergence dates. Overall accuracy for each quantile is calculated correspondingly for the three testing years. As the accuracy reaches plateau near the end of September (see Fig. 6), we use the overall accuracy at that time as an example to demonstrate how the model performances respond to crop emergence dates.

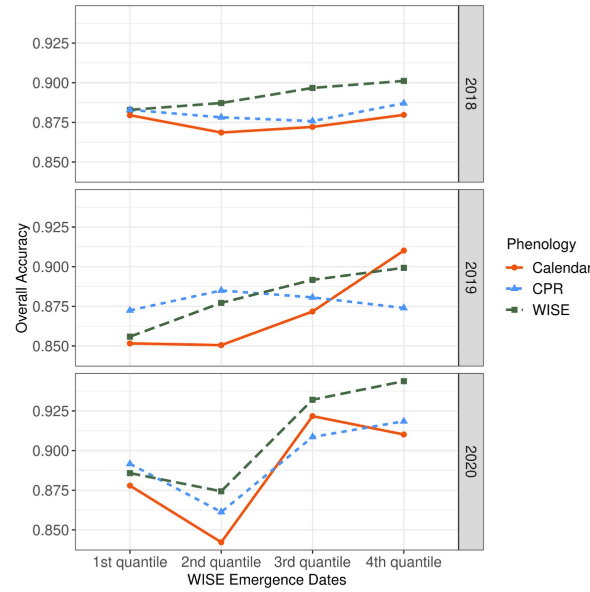

Fig. 10. Overall accuracy of the pure pixels across the four quantiles of WISE-derived crop emergence dates by the end of September in 2018, 2019, and 2020, with 2017 as the training year.

Fig. 10 indicates that the WISE-phenology normalized model generally performs better than the other two models across different quantiles. In addition, the proposed model tends to exhibit better performance for pixels with later emergence dates in all the three testing years. To test whether the performance of our proposed model is related to crop emergence dates, all the pure pixels are labeled using two categorical variables, namely which quantile they belong to (first categorical variable) and whether they are correctly classified (second categorical variable). Chi-squared tests are conducted between these two variables, and the results suggest that the model performance is positively associated with the detected crop emergence dates in all the three testing years ($p = 0.024$ in 2018, $p < 0.001$ in 2019 and 2020). This association could possibly be attributed to the confusion between signals of weeds growth and those of crop emergence at the early season. While the WISE algorithm incorporates the momentum criteria to ensure the significance of detected green-up signals, there may still exist circumstances where the detected green-up may be caused by the signals other than that of crop emergence. For example, when the crop is planted late, weeds may have grown for a long time before crop emergence. Such strong weeds growth signals might potentially meet the momentum criteria and result in earlier WISE-detected crop emergence dates.

C. Model Performances Across ASDs and Years

Fig. 11 shows the CV of overall accuracy among the nine ASDs in Illinois throughout the growing season in 2018, 2019, and 2020, with 2017 as the training year. Lower CV values suggest that the model performs more stably across the ASDs with different climatic conditions, indicating higher model

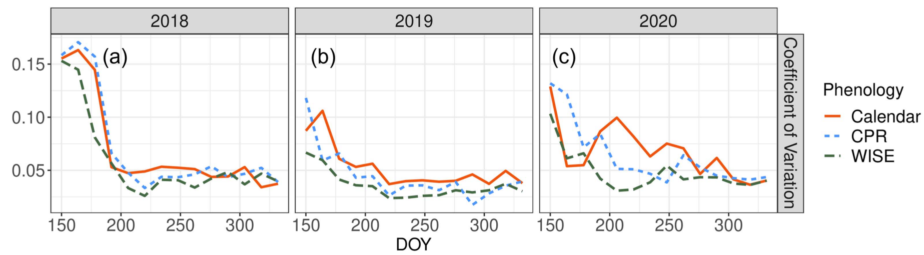

Fig. 11. Coefficient of variation (CV) of the overall accuracy across the nine ASDs in Illinois throughout the growing season in (a) 2018, (b) 2019, and (c) 2020.

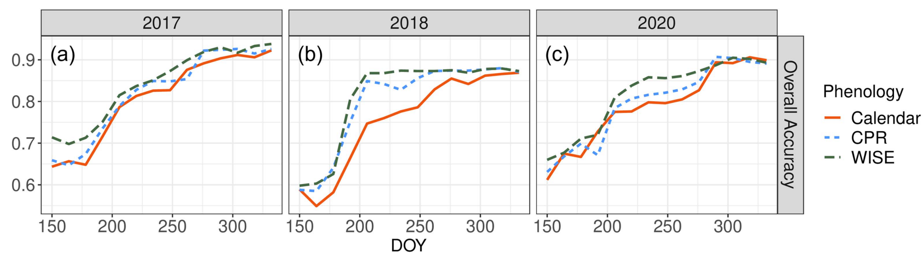

Fig. 12. Overall accuracy of the crop classification result throughout the growing season in (a) 2017, (b) 2018, and (c) 2020, with 2019 as the training year.

scalability. Overall, the CV values tend to be higher at the beginning of the growing season under the three devised approaches. As the growing season progresses and longer time-series data are utilized, the model performance gets more stabilized. In all the three testing years, the calendar-based approach tends to generate higher CV values compared to the other two approaches, while the proposed model generally yields the lowest CV values. In summary, the results suggest that the WISE-phenology normalized model performs more stably than the other two models, and can be applied across ASDs with great scalability.

To further evaluate the temporal transferability of the WISE-phenology normalized model, we train our model using the data in 2019 when abnormal extreme precipitation events in spring caused delayed crop planting. Fig. 1(c) suggests that the crop in 2019 possesses a significantly different phenology pattern compared to that of the other years. Fig. 12 shows the overall accuracy of the crop mapping results throughout the growing season in 2017, 2018, and 2020. Our proposed model again achieves generally higher overall accuracy compared to the other two models in all the three testing years. Compared to Fig. 6(a)–(c), which are generated from the models trained with 2017 data, the accuracy difference between the calendar-based model and the other two models tends to be relatively larger, especially in the year of 2018 in which the crop emergence progress is the most different from that in 2019. This test of using an extreme year as training data further supports the effectiveness of the proposed WISE-phenology normalization approach in scalable within-season crop mapping across years.

V. Discussion

In this article, we propose to incorporate WISE-derived phenology into a At1DCNN model in an effort to enhance the model scalability for within-season crop mapping. The At1DCNN model, built upon the TempCNN blocks and the attention module, can effectively extract and learn complex temporal features from the dense satellite time-series data. With the WISE-derived phenology, the At1DCNN model demonstrates good performance in estimating the crop types within the growing season by leveraging other years' remote sensing and crop type reference data for model building. The experiment results indicate that the WISE-phenology normalized model achieves higher classification accuracy and better model transferability compared to the calendar-based model and CPR normalized model (see Fig. 6). Such improvements in model performance are largely attributed to the incorporation of WISE-derived phenology, which enables the deep learning classifier to better accommodate the variations in crop phenological progress over space and time.

Conventionally, within-season crop mapping has been mostly explored through calendar-based modeling approaches without the consideration of the spatiotemporal variations in crop phenology, hampering the model transferability across years and regions [18], [21]. The advances in remote sensing have opened up new opportunities for large-scale characterization and normalization of pixel-level crop phenology. Kerner et al. [26] recently accommodated and normalized the crop phenological variation at the pixel level by using the spectral information acquired at three key phenological stage transition dates (i.e., greenup, peak, and senescence). With the spectral information normalized via those transition dates, the in-season classification of corn and soybean was found to be improved in the central U.S. Corn Belt. Similarly, the improved performance of crop mapping has also been found in our study with phenology normalization. In this article, we normalize the pixel-level crop phenological variation using the WISE model. With the timely and accurate characterization of crop emergence stage, the WISE model enables more frequent weekly update of crop type mapping throughout the growing season using the dense satellite time-series. Through the WISE-phenology normalization approach, the deep learning classifier can be better adapted to the spatiotemporal variability in crop phenology and learn the temporal features embedded in the dense time-series sequence more effectively.

The advantages of leveraging the WISE model for phenological normalization mainly lie in two aspects. First, the WISE model is able to characterize the crop emergence stage more accurately than most conventional remote-sensing phenology methods. Previous studies indicate that conventional remote sensing phenology methods tend to characterize land surface phenology, which may not be directly associated with ground-observed crop phenological stages. Compared to conventional phenology methods which typically detect the V3-V4 crop vegetative stages (three to four leaves observed, typically two to four weeks after ground-observed crop emergence), WISE can capture crop emergence within approximately five days after the ground-observed VE (emergence) to V1 (one leaf) stages of corn and the VE (emergence) to VC (unrolled unifoliolate leaves) stages of soybeans [27], [28]. The general agreement between the cumulative distribution of WISE-derived crop emergence dates and that of CPR-based crop emergence dates (see Fig. 4) also demonstrates the efficacy of the WISE model. As a result, the incorporation of WISE-derived phenology enables more accurate crop emergence characterization and the subsequent crop type mapping during the growing season.

Another advantage held by the WISE model is that it enables near real-time characterization of the crop phenology. The MACD function and the momentum criteria incorporated in the WISE model facilitate the detection of subtle uptrends in the NDVI time series in the early growing season. The WISE model is thus capable of utilizing partial observations during the growing season for near real-time phenology monitoring. Its estimation results can be updated frequently with newly acquired satellite images [27], [37]. Leveraging the WISE-derived phenology information, the WISE-phenology normalized crop mapping model holds the similar advantage. In this article, the WISE-phenology normalized model is designed to utilize within-season partial time series of satellite observations, and results have demonstrated its ability to provide weekly updates of the crop type predictions (see Fig. 6). Coupled with the accurate characterization of crop emergence dates, the proposed model is promising in providing near real-time estimation of crop types with the most up-to-date satellite image data from the early season to the end of the growing season.

The scalability and transferability of the proposed model is examined across Illinois from 2017 to 2020. The study period contains relatively normal years (i.e., 2017 and 2020) and years with extreme weather disturbances (i.e., 2018 and 2019), especially for 2019 with a record wet spring. Through the experimental design of model training in only one year and testing in several other years, we found that both the WISE-phenology normalized model trained with 2017 and 2019 data can be well generalized during the study period. Satisfactory results can also be achieved earlier by the our proposed model than the CPR normalized and calendar-based models (see Table II). Apart from temporal transferability, the proposed model also yields lower CV values across the nine ASDs in Illinois (see Fig. 11), suggesting that a more spatially homogeneous performance is achieved by the proposed model. In summary, the WISE-phenology normalized model outperforms the other two models in being generalized across years and regions in Illinois.

Despite the advantages and good performance of the WISE-phenology normalized model, it also has limitations. The WISE-phenology normalization approach mainly focuses on normalizing the early-season crop phenology (i.e., crop emergence stage) across years and districts. As one of the major crop management practices, crop planting timing has significant impacts on the subsequent crop growth patterns and conditions. Yet the crop phenological progress throughout the season might also be subject to the influence of a variety of environmental and human factors (e.g., temperature, precipitation, and farming practices). For instance, the phenology progress affected by droughts or flooding occurrence in the middle of season might not be well captured and normalized by the WISE-phenology normalization approach. The limitation of the ability to timely characterize whole-season phenological stages may bring uncertainties in the current WISE-phenology normalization design. For example, Figs. 6 and 12 suggest that the advantage of our model is more substantial in early- to mid-season, while in late-season the three models tend to perform more similarly. Table I also illustrates that the hypothetically most comparable year of 2020 might not guarantee the highest end-of-season accuracy. Future efforts could be devoted to the timely incorporation of phenology information throughout the whole growing season for building a more comprehensive phenology normalization model. While Illinois encompasses nine ASDs with relatively different climatic conditions, the variation in crop phenological progress across the ASDs of a year is found to be less significant than the interannual variation of the crop phenology [23]. In the future, the proposed WISE-phenology normalization approach could be validated in extended areas across a larger number of climate divisions defined by the U.S. National Oceanic and Atmospheric Administration [42]. With corn and soybeans as the two dominant crop species, the U.S. Corn Belt stands for an ideal study site for crop type mapping. Yet future work can be focused on extending the proposed model to other agricultural production regions where an increased number of crop types and natural vegetation types can be included and tested.

This article employs the MODIS MCD43A4 Version 6 products considering its high temporal resolution with reliable spectral quality. The high temporal resolution of the MODIS data facilitates accurate characterization of crop emergence in the early season. With the increasing availability of satellite image products (e.g., Landsat-9, PlanetScope, and Harmonized Landsat Sentinel-2) and recent advances in satellite spatiotemporal data fusion techniques [43], [44], [45], [46], [47], the proposed modeling strategy can potentially be applied to those fine-resolution datasets to enable operational applications in the future. Such fine-resolution application of the proposed WISE-phenology normalized model could further benefit precision agriculture, which requires agricultural monitoring at field scales.

Within-season crop mapping provides valuable information for a variety of applications ranging from the management of water consumption and pesticides usage, to crop acreage and yield estimation [7], [9], [48]. For the crop market, within-season crop acreage information is essential for relevant governmental agencies to understand and estimate the crop production, supply, and prices [49]. In the US, the USDA survey-based planted acreage reports serve as the benchmark in grain markets [49], [50], [51]. As the timing of those crop reports collected from farmers varies, the survey-based USDA reports of acreage and production estimates are subject to updates and revisions during the growing season. Such revisions made between August and October (mid- to late-season) have been found with critical market impacts and likely result in substantial market volatility [51], [52]. Within-season crop mapping, by supporting timely monitoring and updates of the crop planted acreage, may complement the survey-based planted acreage reports and provide important implications for decision-makers to understand the crop market volatility and make risk management plans. The within-season crop type mapping results could also support a variety of agricultural applications (e.g., the estimation and prediction of crop growth conditions and yields), which could further enhance food security for more sustainable agricultural development.

VI. Conclusion

In this article, an innovative WISE-phenology normalized deep learning model is proposed. Time-series remote sensing data derived from pure MODIS pixels in Illinois are normalized and aligned by each pixel's emergence date estimated by the WISE algorithm. This pixel-level phenology normalization process greatly helps the crop mapping models accommodate the spatiotemporal variations in crop phenological dynamics and growth patterns. Coupled with the At1DCNN model specifically designed for temporal feature learning, the WISE-phenology normalization approach is more effective than the calendar-based and CPR state-level normalization approaches. The WISE-phenology normalized deep learning model exhibits more stable performance across Illinois and demonstrates superior performance both within the growing season and at the end of the growing season. It achieves the 85% overall accuracy earlier than both the calendar-based and CPR normalized ones.

Acknowledgment

The authors would like to thank the MODIS team and USDA NASS for generating the MODIS MCD43A4 and CDL products, respectively, and like to appreciate the constructive and insightful comments from the three anonymous reviewers to help improve the quality of this article.

References

[1] J. Sachs et al., "Monitoring the world's agriculture," *Nature*, vol. 466, no. 7306, pp. 558–560, 2010.
[2] H.-O. Pörtner et al., "Climate change 2022: Impacts, adaptation and vulnerability," in *Proc. IPCC 6th Assessment Rep.*, 2022, pp. 37–118.
[3] A. Y. Prosekov and S. A. Ivanova, "Food security: The challenge of the present," *Geoforum*, vol. 91, pp. 73–77, 2018.
[4] M. Burke and D. B. Lobell, "Satellite-based assessment of yield variation and its determinants in smallholder African systems," *Proc. Nat. Acad. Sci.*, vol. 114, no. 9, pp. 2189–2194, 2017.
[5] C. Atzberger, "Advances in remote sensing of agriculture: Context description, existing operational monitoring systems and major information needs," *Remote Sens.*, vol. 5, no. 2, pp. 949–981, 2013.
[6] A. Bégué et al., "Remote sensing and cropping practices: A review," *Remote Sens.*, vol. 10, no. 1, 2018, Art. no. 99.
[7] X. Liu et al., "Large-scale crop mapping from multisource remote sensing images in Google earth engine," *IEEE J. Sel. Topics Appl. Earth Observ. Remote Sens.*, vol. 13, pp. 414–427, 2020.
[8] D. B. Lobell, D. Thau, C. Seifert, E. Engle, and B. Little, "A scalable satellite-based crop yield mapper," *Remote Sens. Environ.*, vol. 164, pp. 324–333, 2015.
[9] Y. Cai et al., "A high-performance and in-season classification system of field-level crop types using time-series landsat data and a machine learning approach," *Remote Sens. Environ.*, vol. 210, pp. 35–47, 2018, doi: 10.1016/j.rse.2018.02.045.
[10] Y. LeCun, Y. Bengio, and G. Hinton, "Deep learning," *Nature*, vol. 521, no. 7553, pp. 436–444, May 2015, doi: 10.1038/nature14539.
[11] Q. Yuan et al., "Deep learning in environmental remote sensing: Achievements and challenges," *Remote Sens. Environ.*, vol. 241, 2020, Art. no. 111716.
[12] L. Ma, Y. Liu, X. Zhang, Y. Ye, G. Yin, and B. A. Johnson, "Deep learning in remote sensing applications: A meta-analysis and review," *ISPRS J. Photogrammetry Remote Sens.*, vol. 152, pp. 166–177, 2019, doi: 10.1016/j.isprsjprs.2019.04.015.
[13] M. Rußwurm and M. Körner, "Self-attention for raw optical satellite time series classification," *ISPRS J. Photogrammetry Remote Sens.*, vol. 169, pp. 421–435, 2020.
[14] C. Pelletier, G. I. Webb, and F. Petitjean, "Temporal convolutional neural network for the classification of satellite image time series," *Remote Sens.*, vol. 11, no. 5, 2019, Art. no. 523.
[15] L. Zhong, L. Hu, H. Zhou, and X. Tao, "Deep learning based winter wheat mapping using statistical data as ground references in Kansas and northern Texas, US," *Remote Sens. Environ.*, vol. 233, 2019, Art. no. 111411, doi: 10.1016/j.rse.2019.111411.
[16] L. Zhong, L. Hu, and H. Zhou, "Deep learning based multi-temporal crop classification," *Remote Sens. Environ.*, vol. 221, pp. 430–443, 2019, doi: 10.1016/j.rse.2018.11.032.
[17] N. Kussul, M. Lavreniuk, S. Skakun, and A. Shelestov, "Deep learning classification of land cover and crop types using remote sensing data," *IEEE Geosci. Remote Sens. Lett.*, vol. 14, no. 5, pp. 778–782, May 2017.
[18] J. Xu et al., "DeepCropMapping: A multi-temporal deep learning approach with improved spatial generalizability for dynamic corn and soybean mapping," *Remote Sens. Environ.*, vol. 247, 2020, Art. no. 111946.
[19] S. Wang, G. Azzari, and D. B. Lobell, "Crop type mapping without field-level labels: Random forest transfer and unsupervised clustering techniques," *Remote Sens. Environ.*, vol. 222, pp. 303–317, 2019.
[20] R. Yaramasu, V. Bandaru, and K. Pnvr, "Pre-season crop type mapping using deep neural networks," *Comput. Electron. Agriculture*, vol. 176, 2020, Art. no. 105664.
[21] D. M. Johnson and R. Mueller, "Pre-and within-season crop type classification trained with archival land cover information," *Remote Sens. Environ.*, vol. 264, 2021, Art. no. 112576.
[22] R. Azar, P. Villa, D. Stroppiana, A. Crema, M. Boschetti, and P. A. Brivio, "Assessing in-season crop classification performance using satellite data: A test case in Northern Italy," *Eur. J. Remote Sens.*, vol. 49, no. 1, pp. 361–380, 2016.
[23] C. Diao, Z. Yang, F. Gao, X. Zhang, and Z. Yang, "Hybrid phenology matching model for robust crop phenological retrieval," *ISPRS J. Photogrammetry Remote Sens.*, vol. 181, pp. 308–326, 2021.
[24] L. Zeng et al., "A hybrid approach for detecting corn and soybean phenology with time-series MODIS data," *Remote Sens. Environ.*, vol. 181, pp. 237–250, 2016.
[25] L. Zhong, P. Gong, and G. S. Biging, "Efficient corn and soybean mapping with temporal extendability: A multi-year experiment using landsat imagery," *Remote Sens. Environ.*, vol. 140, pp. 1–13, 2014.
[26] H. R. Kerner et al., "Phenological normalization can improve in-season classification of maize and soybean: A case study in the central US corn belt," *Sci. Remote Sens.*, vol. 6, 2022, Art. no. 100059.
[27] F. Gao, M. Anderson, C. Daughtry, A. Karnieli, D. Hively, and W. Kustas, "A within-season approach for detecting early growth stages in corn and soybean using high temporal and spatial resolution imagery," *Remote Sens. Environ.*, vol. 242, 2020, Art. no. 111752.

[28] F. Gao et al., "Towards routine mapping of crop emergence within the season using the harmonized landsat and sentinel-2 dataset," *Remote Sens.*, vol. 13, no. 24, 2021, Art. no. 5074.
[29] P. S. Beck, C. Atzberger, K. A. Høgda, B. Johansen, and A. K. Skidmore, "Improved monitoring of vegetation dynamics at very high latitudes: A new method using MODIS NDVI," *Remote Sens. Environ.*, vol. 100, no. 3, pp. 321–334, 2006.
[30] C. Diao, "Remote sensing phenological monitoring framework to characterize corn and soybean physiological growing stages," *Remote Sens. Environ.*, vol. 248, 2020, Art. no. 111960.
[31] X. Zhang et al., "Monitoring vegetation phenology using MODIS," *Remote Sens. Environ.*, vol. 84, no. 3, pp. 471–475, 2003.
[32] X. Zhang et al., "Generation and evaluation of the VIIRS land surface phenology product," *Remote Sens. Environ.*, vol. 216, pp. 212–229, 2018.
[33] L. Liu et al., "Detecting crop phenology from vegetation index time-series data by improved shape model fitting in each phenological stage," *Remote Sens. Environ.*, vol. 277, 2022, Art. no. 113060.
[34] T. Sakamoto, B. D. Wardlow, A. A. Gitelson, S. B. Verma, A. E. Suyker, and T. J. Arkebauer, "A two-step filtering approach for detecting maize and soybean phenology with time-series MODIS data," *Remote Sens. Environ.*, vol. 114, no. 10, pp. 2146–2159, 2010, doi: 10.1016/j.rse.2010.04.019.
[35] C. Diao and G. Li, "Near-surface and high-resolution satellite time series for detecting crop phenology," *Remote Sens.*, vol. 14, no. 9, 2022, Art. no. 1957.
[36] C. Diao, "Innovative pheno-network model in estimating crop phenological stages with satellite time series," *ISPRS J. Photogrammetry Remote Sens.*, vol. 153, pp. 96–109, 2019.
[37] F. Gao and X. Zhang, "Mapping crop phenology in near real-time using satellite remote sensing: Challenges and opportunities," *J. Remote Sens.*, vol. 2021, 2021, doi: 10.34133/2021/8379391.
[38] C. Boryan, Z. Yang, R. Mueller, and M. Craig, "Monitoring US agriculture: The US department of agriculture, national agricultural statistics service, cropland data layer program," *Geocarto Int.*, vol. 26, no. 5, pp. 341–358, 2011.
[39] USDA-NASS. Accessed: Apr. 1, 2022. [Online]. Available: https://www.nass.usda.gov/Publications/National_Crop_Progress/
[40] G. Appel, *Technical Analysis: Power Tools for Active Investors*. Upper Saddle River, NJ, USA: FT Press, 2005.
[41] G. M. Foody, "Explaining the unsuitability of the kappa coefficient in the assessment and comparison of the accuracy of thematic maps obtained by image classification," *Remote Sens. Environ.*, vol. 239, 2020, Art. no. 111630.
[42] R. S. Vose et al., "Improved historical temperature and precipitation time series for US climate divisions," *J. Appl. Meteorol. Climatol.*, vol. 53, no. 5, pp. 1232–1251, 2014.
[43] P. Wang, F. Gao, and J. G. Masek, "Operational data fusion framework for building frequent landsat-like imagery," *IEEE Trans. Geosci. Remote Sens.*, vol. 52, no. 11, pp. 7353–7365, Nov. 2014, doi: 10.1109/tgrs.2014.2311445.
[44] C. Liao, J. Wang, T. Dong, J. Shang, J. Liu, and Y. Song, "Using spatio-temporal fusion of landsat-8 and MODIS data to derive phenology, biomass and yield estimates for corn and soybean," *Sci. Total Environ.*, vol. 650, pp. 1707–1721, 2019.
[45] Z. Yang, C. Diao, and B. Li, "A robust hybrid deep learning model for spatiotemporal image fusion," *Remote Sens.*, vol. 13, no. 24, 2021, Art. no. 5005.
[46] F. Gao et al., "Toward mapping crop progress at field scales through fusion of landsat and MODIS imagery," *Remote Sens. Environ.*, vol. 188, pp. 9–25, 2017, doi: 10.1016/j.rse.2016.11.004.
[47] Z. Tan, M. Gao, X. Li, and L. Jiang, "A flexible reference-insensitive spatiotemporal fusion model for remote sensing images using conditional generative adversarial network," *IEEE Trans. Geosci. Remote Sens.*, vol. 60, 2022, Art. no. 5601413.
[48] G. Fontanelli et al., "Early-season crop mapping on an agricultural area in Italy using X-band dual-polarization SAR satellite data and convolutional neural networks," *IEEE J. Sel. Toics Appl. Earth Observ. Remote Sens.*, vol. 15, pp. 6789–6803, 2022.
[49] B. Karali, O. Isengildina-Massa, S. H. Irwin, M. K. Adjemian, and R. Johansson, "Are USDA reports still news to changing crop markets?," *Food Policy*, vol. 84, pp. 66–76, 2019.
[50] O. Isengildina-Massa, B. Karali, and S. H. Irwin, "Can private forecasters beat the USDA? Analysis of relative accuracy of crop acreage and production forecasts," *J. Agricultural Appl. Econ.*, vol. 52, no. 4, pp. 545–561, 2020.
[51] O. Isengildina-Massa, X. Cao, B. Karali, S. H. Irwin, M. Adjemian, and R. C. Johansson, "When does USDA information have the most impact on crop and livestock markets?," *J. Commodity Markets*, vol. 22, 2021, Art. no. 100137.
[52] S. Irwin, "What do we know about revisions to USDA planted acreage estimates?," *Farmdoc Daily*, vol. 12, no. 95, pp. 1–5, 2022.

Zijun Yang received the B.S. degree in geographic information systems from Sun Yat-sen University, Guangzhou, China, in 2016, and the M.S. degree in natural resources and environment from the University of Michigan, Ann Arbor, MI, USA, in 2018. He is currently working toward the Ph.D. degree in geography with the University of Illinois at Urbana-Champaign, Champaign, IL, USA.

He is a Graduate Research Assistant with the University of Illinois at Urbana-Champaign. His research interests include time series remote sensing, spatiotemporal image fusion, and machine learning/deep learning applications in agricultural remote sensing.

Chunyuan Diao received the B.S. degree in resources science and engineering from the Beijing Normal University, Beijing, China, in 2010, and the M.A. degree in biostatistics and the Ph.D. degree in geography from the State University of New York at Buffalo, Buffalo, NY, USA, in 2014 and 2017, respectively.

She is currently an Assistant Professor with the Department of Geography and Geographic Information Science, University of Illinois at Urbana-Champaign, Champaign, IL, USA. Her research is funded by the National Center for Supercomputing Applications, National Science Foundation, and United States Department of Agriculture. Her research interests include the confluence of remote sensing, geographic information science, and biogeography, with current research focusing on computational remote sensing in characterizing land surface patterns and processes, underlying mechanisms, and responses to climate change and human activities.

Dr. Diao was the recipient of several awards for her research, including the NSF CAREER award, the Early Career Scholars in Remote Sensing Award from the AAG Remote Sensing Specialty Group, and the Microsoft AI for Earth Award.

Feng Gao received the B.A. degree in geology and the M.E. degree in remote sensing from Zhejiang University, Hangzhou, China, in 1989 and 1992, respectively, the Ph.D. degree in geography from Beijing Normal University, Beijing, China, in 1998, and the M.S. degree in computer science from Boston University, Boston, MA, USA, in 2003.

From 1992 to 1998, he was a Research Assistant with the Nanjing Institute of Geography and Limnology, Chinese Academy of Science, Nanjing, China. From 1998 to 2004, he was a Researcher with the Department of Geography, Center for Remote Sensing, Boston University. From 2004 to 2011, he was a Research Scientist with Earth Resources Technology, Inc. and the NASA Goddard Space Flight Center. Since 2011, he has been a Research Physical Scientist with the Hydrology and Remote Sensing Laboratory, USDA Agricultural Research Service. He has authored or coauthored more than 160 publications in peer-reviewed journals. His recent research interests include crop phenology, water use, and yield mapping using multisensor remote sensing data fusion at field scales.

Dr. Gao has been selected to serve on Landsat and MODIS Science Teams. He developed many high-impact remote sensing tools (e.g., STARFM, AROP) that are openly available to the remote sensing community. He received the 2018 Arthur Flemming Award as an exceptional federal employee for his original research in applying remote sensing for crop and vegetation monitoring.